

Supporting Information

Unveiling the Role of Ground State Charge Transfer Complex in Carbon Nanoparticles for Highly Efficient Metal-free Solar Hydrogen Production

Subhajit Kar¹, Amit Kumar², Ramesh Mandal¹, Sakshi Chawla², Shanti Gopal Patra³, Arijit De^{2*}, and Santanu Bhattacharyya^{1*}

¹Department of Chemical Sciences, Indian Institute of Science Education and Research Berhampur, Berhampur, Odisha-760010, India.

²Condensed Phase Dynamics Group, Department of Chemical Sciences, Indian Institute of Science Education and Research Mohali, SAS Nagar, Punjab 140306, India.

³Department of Chemistry, National Institute of Technology Silchar, Silchar, 788010, India.

*- Corresponding authors: E-mail:

A.D - akde@iisermohali.ac.in, S.B.- santanub@iiserbpr.ac.in

Contents:

SI. Single Wavelength Analysis (fs-TA) for 400 nm Pump.

SII. Single Wavelength Analysis for 530 nm Pump.

SIII. Fluorescence Lifetime Studies.

SIV. Detailed Characterization

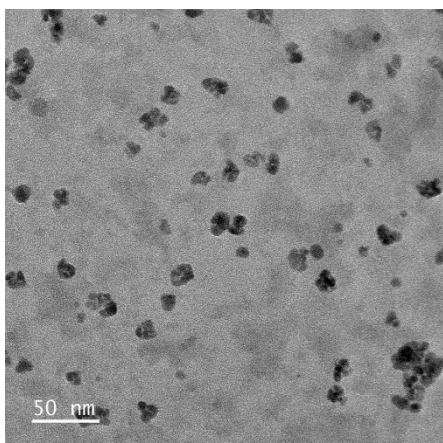


Fig-S1: HRTEM image of N, P-CNPs at relatively lower resolutions.

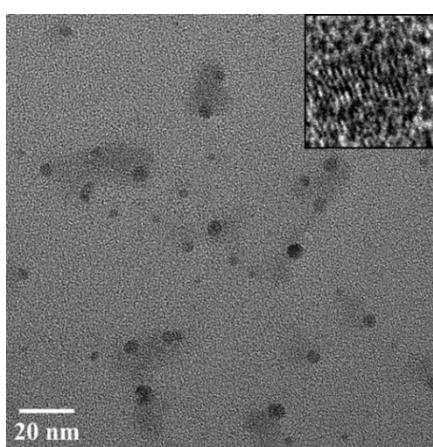


Fig-S2: HRTEM image of N-CDs.

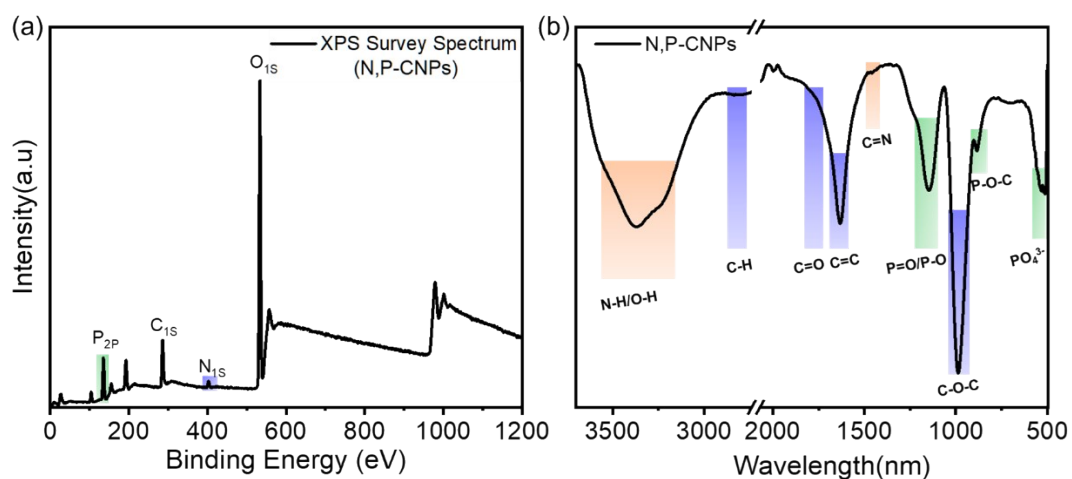


Fig-S3: XPS survey spectra (a) and FTIR spectra (b) of N, P-CNPs.

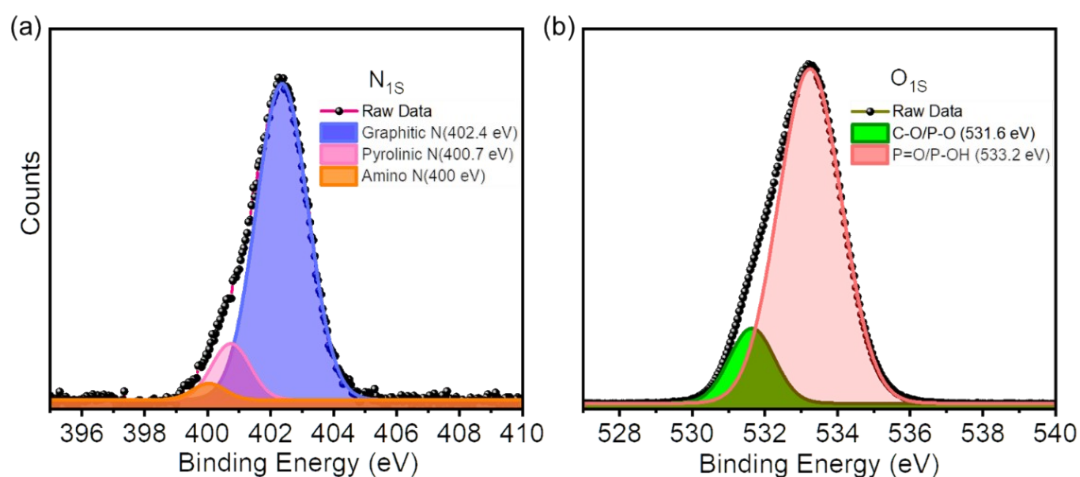


Fig-S4: Deconvoluted XPS spectra of N, P-CNPs: (a) high-resolution N_{1s} and O_{1s} spectra (b) respectively.

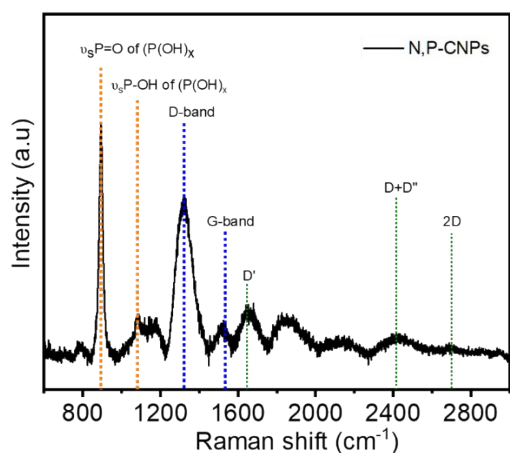


Fig-S5: Raman spectra of as-synthesized N, P-CNPs.

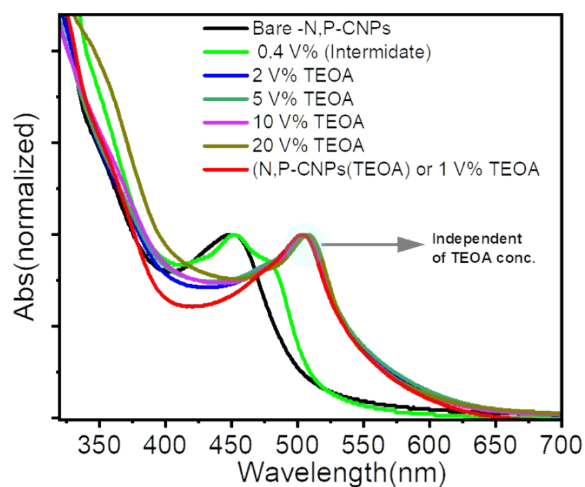


Fig-S6: UV-Vis absorption spectra (normalized) of N, P-CNPs with increasing TEOA concentration.

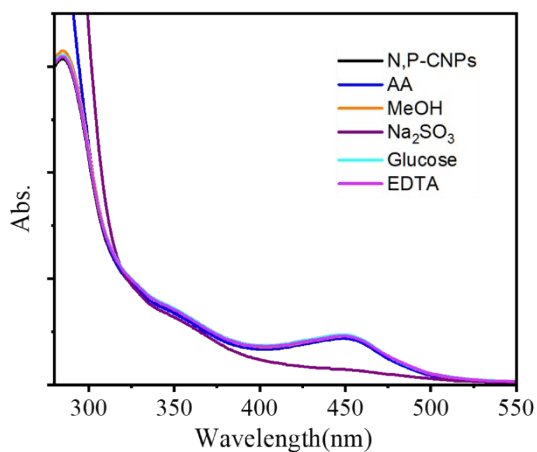


Fig-S7: UV-Vis absorption spectra of pure N, P-CNPs, and upon addition of common SEDs.

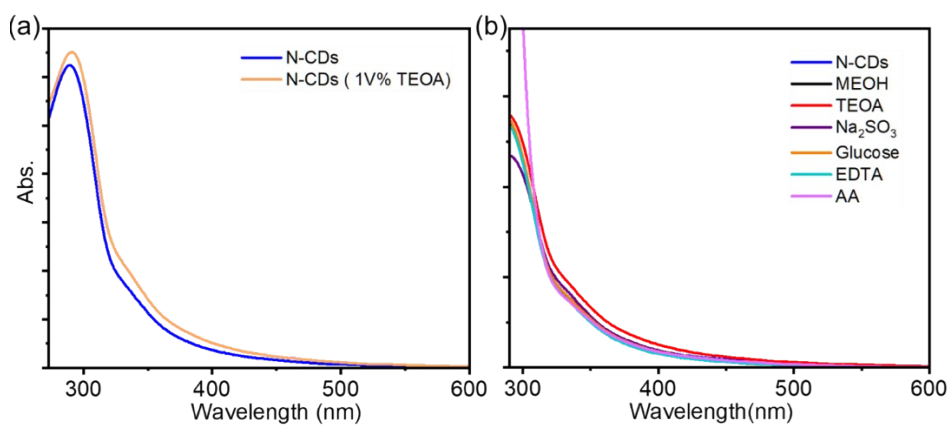


Fig-S8: UV-Vis absorption spectra of pure N-CDs and upon TEOA (1V %) addition (a). UV-Vis absorption spectra of N-CDs upon common SEDs addition (b).

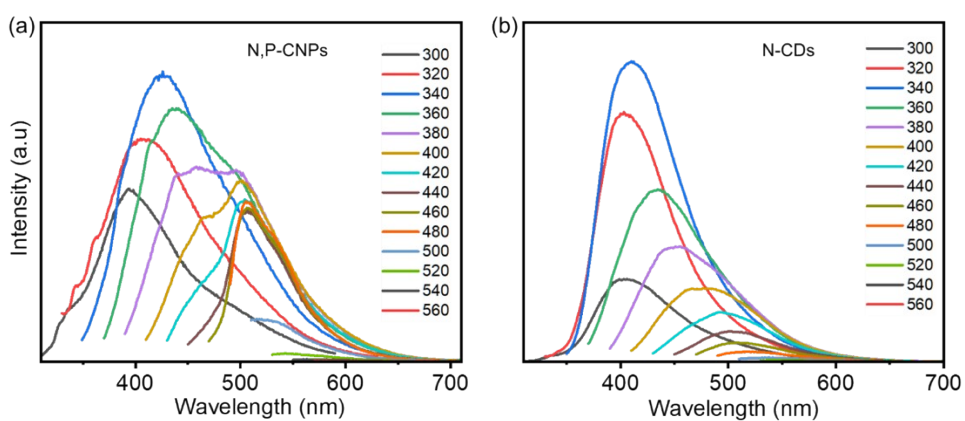


Fig-S9: Steady state PL emission spectra N, P-CNPs (a), and pure N-CDs (b) respectively.

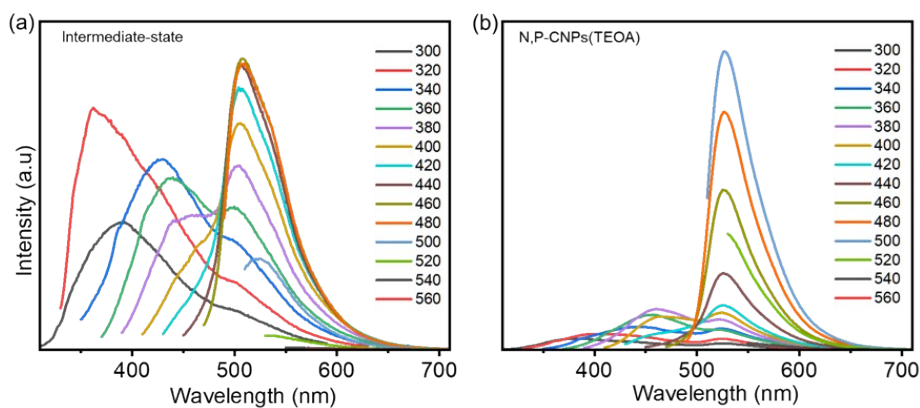


Fig-S10: Steady state PL emission spectra of intermediate state between *N*, *P*-CNPs, and TEOA (0.4V % TEOA) (a), and fully complexed *N*, *P*-CNPs (TEOA) adduct (1V % TEOA) (b).

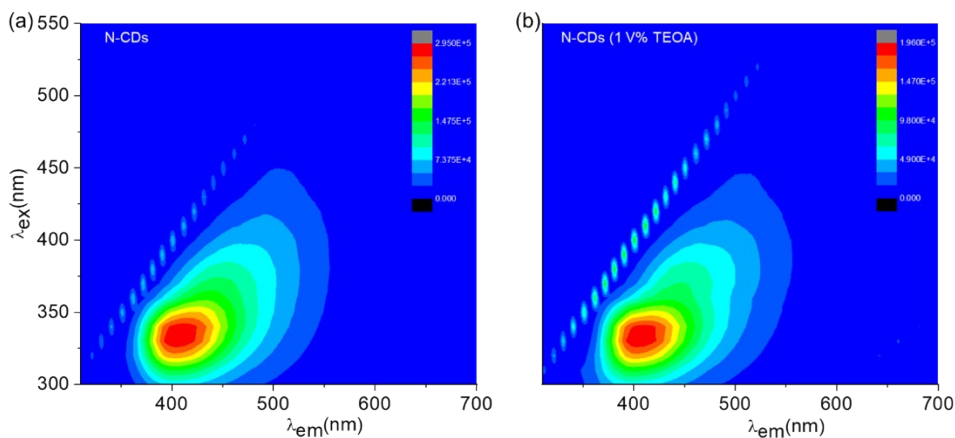


Fig-S11: Steady state PL emission spectra bare *N*-CDs (a) and *N*-CDs in the presence of TEOA (1V %) (b).

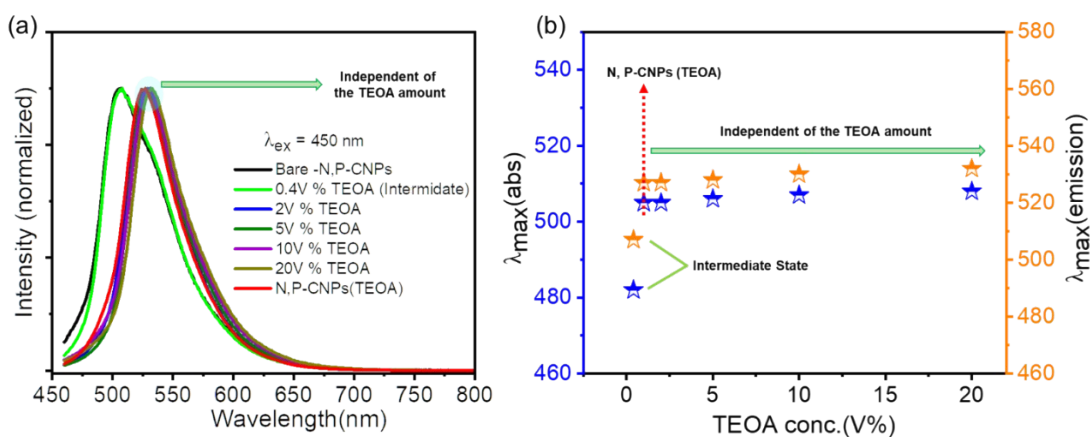


Fig-S12: PL emission ($\lambda_{ex} = 450 \text{ nm}$) spectra (normalized) of *N*, *P*-CNPs with increasing TEOA concentration (a). Location of absorption maxima and PL emission maxima ($\lambda_{ex} = 450 \text{ nm}$) Vs. TEOA amount in *N*, *P*-CNPs (b).

Sample Name	$\lambda_{\text{ex}}(\text{nm})$	α_1	α_2	τ_1	τ_2	τ_{avg}
N, P-CNPs	450	0.89	0.11	0.44	1.81	0.59
N, P-CNPs (TEOA)	450	0.92	0.08	2.11	8.84	2.70

Table-S1: Parameters of time-resolved fluorescence lifetime of N, P-CNPs & N, P CNPs (TEOA) data fitted with bi-exponential decay kinetics.

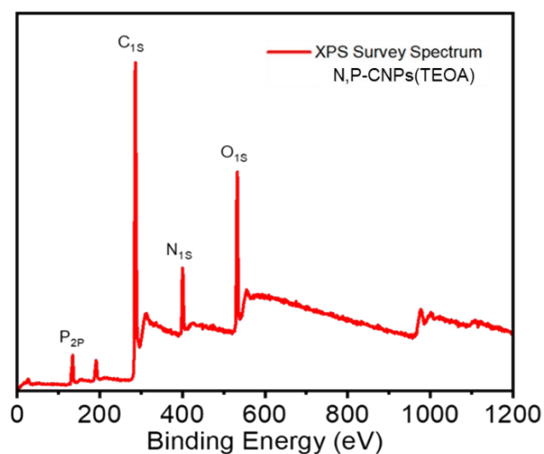


Fig-S13: XPS survey spectra of N, P-CNPs (TEOA).

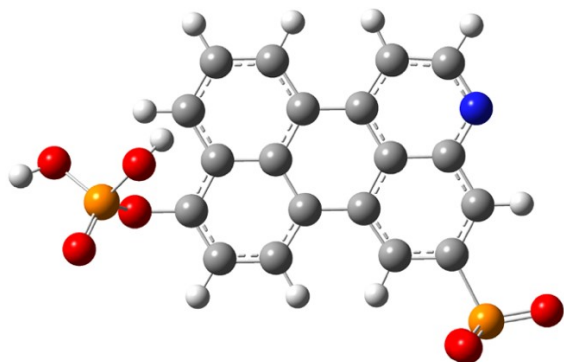


Fig-S14: Ball sticks representation of model N, P-CNPs (TEOA) revealing the state of N, P-CNPs after complexation with TEOA.

Center Number	Atomic Number	Atomic Type	Coordinates (Angstroms)		
			X	Y	Z
1	6	0	2.662960	3.983775	0.387988

2	6	0	1.291828	3.764208	0.210172
3	6	0	0.822300	2.449924	0.028190
4	6	0	3.181159	1.744884	0.225631
5	6	0	-0.586191	2.127809	-0.177125
6	6	0	1.420252	0.030470	-0.125783
7	6	0	0.004492	-0.299927	-0.300594
8	6	0	-0.972148	0.753490	-0.341974
9	6	0	-0.440827	-1.628363	-0.424771
10	6	0	2.429745	-0.937243	-0.116728
11	6	0	3.799964	-0.620383	0.055624
12	6	0	4.151386	0.709259	0.226892
13	1	0	5.203408	0.969270	0.363708
14	1	0	3.019534	5.015975	0.530674
15	6	0	-1.581583	3.125787	-0.218873
16	6	0	-2.922198	2.810823	-0.441093
17	6	0	-3.330890	1.489727	-0.609504
18	6	0	-2.365571	0.439383	-0.547534
19	1	0	-3.661933	3.615684	-0.499539
20	6	0	-1.794394	-1.938693	-0.582680
21	1	0	-2.130176	-2.975501	-0.652893
22	6	0	-2.731867	-0.923759	-0.649794
23	6	0	1.788864	1.404632	0.041210
24	7	0	3.586705	3.036650	0.397143
25	1	0	-4.362614	1.260310	-0.882137
26	8	0	-4.095800	-1.238595	-0.812832
27	15	0	-5.144525	-1.295562	0.413286
28	8	0	-4.586686	-0.273611	1.515695
29	8	0	-5.536050	-2.614448	0.961203
30	8	0	-6.410365	-0.540912	-0.294862
31	1	0	-7.198439	-1.067573	-0.102564
32	1	0	-4.094564	0.483489	1.125680
33	1	0	0.284117	-2.439591	-0.382331
34	1	0	-1.299984	4.170576	-0.088495
35	1	0	2.199990	-1.994778	-0.250947
36	1	0	0.612800	4.617929	0.215455

37	15	0	4.996784	-2.055765	0.028401
38	8	0	4.459988	-2.907060	1.199483
39	8	0	6.404580	-1.476367	0.225130
40	8	0	4.711002	-2.643662	-1.370998

Table-S2: Coordinates of the optimized geometries of *N, P*-CNPs (TEOA) model.

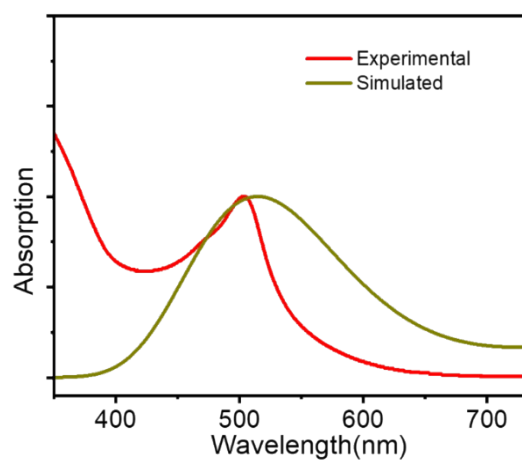


Fig-S15: Comparison of theoretical and experimental UV-visible absorption data (normalized) of model *N, P*-CNPs (TEOA).

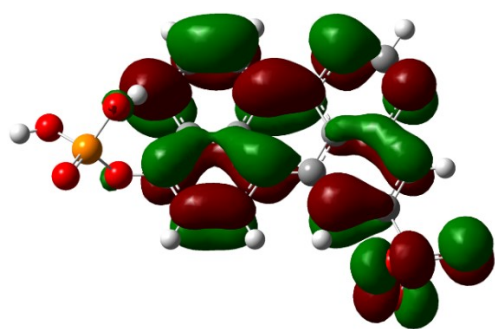


Fig-S16: Representation of LUMO of model *N, P*-CNPs (TEOA).

Femtosecond transient absorption spectroscopy (fs-TAS)

To examine ultrafast charge carrier relaxation dynamics, pump-probe spectroscopy was employed. A custom femtosecond transient-absorption spectroscopy setup from Newport Corp. was employed. In summary, an ultrashort pulse centered at 800 nm was generated by a Ti: sapphire regenerative amplifier (Libra, Coherent Inc.) with a repetition rate of 1 kHz and a pulse width of 55 fs. Then, this pulse was divided into pump and probe pulses using ultrafast beam splitters. A type I -barium borate (BBO) crystal was used to frequency-double the 800 nm output to produce the 400 nm pump pulse. A commercially available non-collinear optical parametric amplifier (NOPA) (TOPAS, Light Conversion) was used to obtain the 530 nm pulse. A portion of the amplified laser output was focused on a CaF₂ crystal to produce a time-delayed broadband white light continuum. This continuum served as a probe in the experiment. To obtain a differential time-resolved transient absorption (ΔOD) for each pump-probe delay, a mechanical chopper (New Focus 3502, Newport Corp.) was used to block the alternate pump pulses at 500 Hz.

SI. Single wavelength analysis for 400 nm pump:

The single wavelength kinetic fitting is performed at the maxima of each signal to reveal the decay dynamics corresponding to different relaxation processes. The kinetic fitting at the selected wavelengths for the 400 nm pump is shown for pure N,P-CNPs in figure SV-(i) (a) , N,P-CNPs(TEOA) or 1V% TEOA (figure SV-(i) (b)), 2V% and 5V% TEOA in figure SV-(i) (c-d). In pure N,P-CNPs, three-time components are obtained by fitting the kinetic traces at 460 and 510 nm. The fastest time component (τ_1) corresponds to the hot charge carrier relaxation, the intermediate time component (τ_2) corresponds to the transfer of population to an emissive state in N,P-CNPs, and the slower time component is related to the charge recombination. However, after the addition of TEOA, the ESA at 450 nm signal is fitted with two exponentials, with the fastest component (τ_1) related to charge relaxation and the slowest component (τ_2) corresponding to charge recombination. In contrast, the ESA signal at 690 nm

decays is fitted with three exponentials with a fast component (τ_1) due to hot charge carrier relaxation, an intermediate time component (τ_2) due to transfer of population to charge separated state a longer component (τ_3) that corresponds to charge recombination. A similar kinetic model is used for the other two samples with more concentration of TEOA (2-5V%).

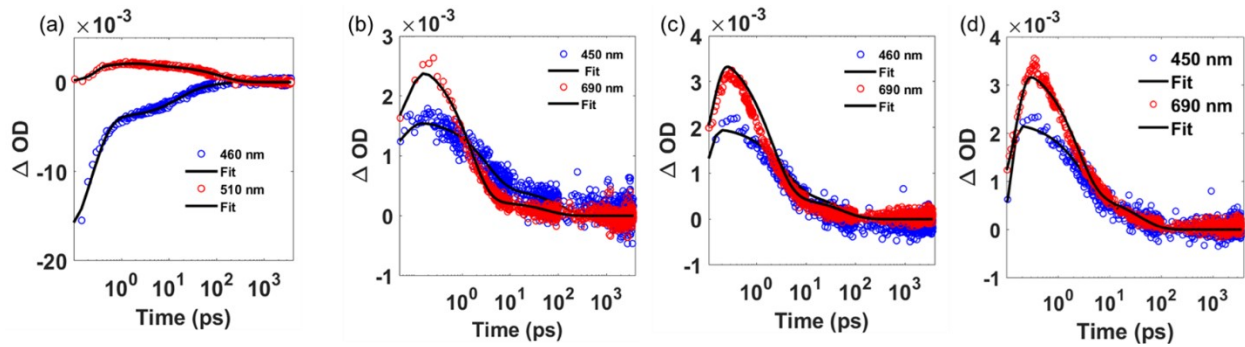


Figure- SI(i): Single wavelength kinetic traces ($\lambda_{pump}=400$ nm): along with fit (in black) to raw data (in scatter) at a selected wavelength for (a) Pure N, P-CNPs, (b) 1V% TEOA, (c) 2V% TEOA, and (d) 5V% TEOA.

SII. Single wavelength analysis for 530 nm pump:

Single wavelength kinetic fitting is performed at the maxima of each signal (430 nm and 519 nm) using three exponentials. For ESA at 519 nm, the fastest time component (τ_1) is related to the initial hot charge carrier relaxation. The intermediate time component (τ_2) corresponds to the transfer of the population to the charge-separated state. Finally, the slowest time component (τ_3) is related to charge recombination. ESA signal at 430 nm is also fitted with three exponentials. The single-wavelength kinetic trace and the corresponding fitting are depicted in figure SVII(i) for N,P-CNPs(TEOA) or 1V%, 2V%, and 5V% TEOA.

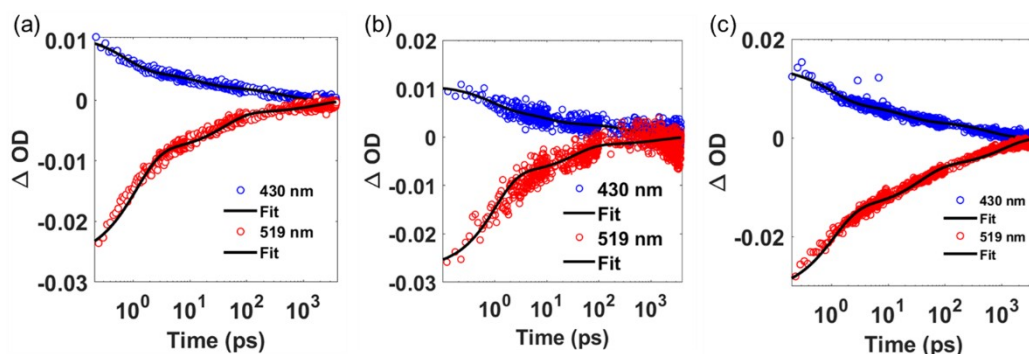


Figure S11(i): Single wavelength kinetic traces ($\lambda_{pump}=530$ nm): along with fit (in black) to raw data (in scatter) at selected wavelength for (a) *N, P*-CNPs(TEOA) or 1V% TEOA, (b) 2V% TEOA, and (c) 5V% TEOA.

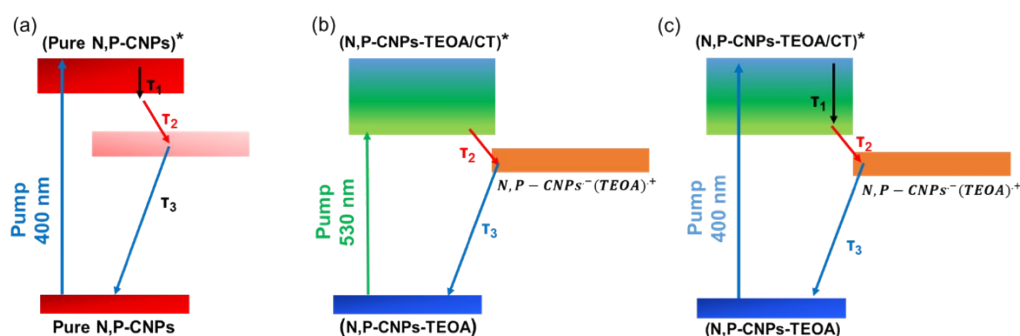


Fig-S17: Proposed kinetic model for pure (a) *N, P*-CNPs and (b, c) *N, P*-CNPs (TEOA) complex involving multi-relaxation pathways corresponding to charge separation and recombination.

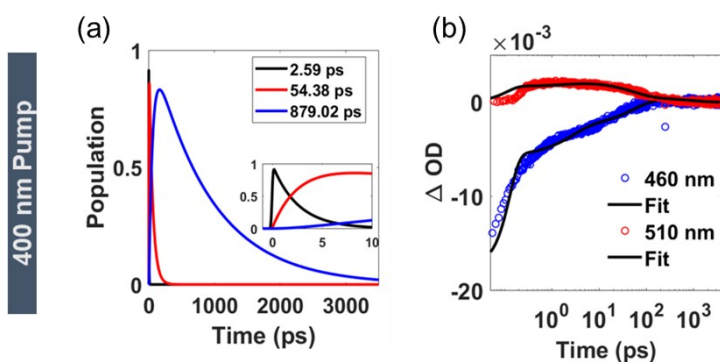


Figure-S18: Femtosecond transient absorption studies of pure *N, P*-CNPs, (a) time evolution population, and (b) kinetic traces along with fit (in black) to raw data (in scatter) at different select probe wavelengths.

Sample	Signal/Wavelength (nm)	α_1	τ_1 (ps)	α_2	τ_2 (ps)	α_3	τ_3 (ps)	RMS
Pure N, P-CNPs	GSB (450)	0.74	0.20	0.12	15.5	0.14	79.9	0.98
	ESA (510)	0.21	0.70	0.17	4.27	0.62	128.6	0.98

Table- S3: TA kinetic fit parameters at the different probe wavelengths for 400 nm excitation.

Sample	Signal/Wavelength h (nm)	α_1	τ_1 (ps)	α_2	τ_2 (ps)	α_3	τ_3 (ps)	RMS
N, P-CNPs(TEOA) (530 nm pump)	ESA (430)	0.54	0.72	0.25	14.08	0.21	457.60	0.96
	GSB+SE (519)	0.66	1.12	0.25	40.23	0.08	1909.0	0.94
N, P-CNPs(TEOA) (400 nm pump)	ESA (450)	0.96	3.30	0.04	110.0	-	-	0.82
	ESA (690)	- 0.014	0.90	0.86	1.62	0.13	176.0	0.92

Table-S4: TA kinetic fit parameters for N, P-CNPs (TEOA) or 1V% TEOA at the different probe wavelengths for 530 and 400 nm excitation.

Sample	Pump wavelength	τ_1 (ps)	τ_2 (ps)	τ_3 (ps)	RMS
Pure N,P-CNPs	400 nm	2.59	54.38	879.0	0.00021
N,P-CNPs(TEOA) or 1%V TEOA	400 nm	0.79	4.45	1940	0.00017
	530 nm	-	6.19	1180	0.00075

Table S5: Kinetic fit parameters of fs-TA data obtained from global analysis.

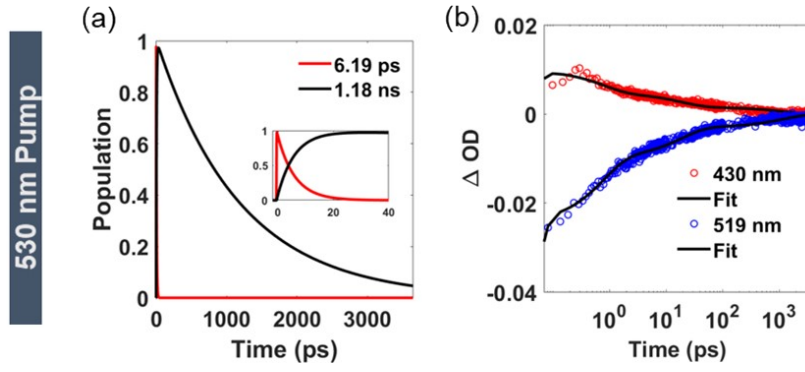


Figure- S19: Femtosecond transient absorption studies of *N, P*-CNPs (TEOA) or 1 V% TEOA, (a) time evolution population and (b) kinetic traces along with fit (in black) to raw data (in scatter) at different select probe wavelengths.

III. Fluorescence lifetime studies:

Fluorescence lifetime measurements are conducted using the Deltaflux system, a commercial time-correlated single photon counting (TCSPC) instrument manufactured by Horiba Scientific. Laser diodes with a central wavelength of 405 nm are utilized for studying pure *N, P*-CNPs, and solutions containing *N, P*-CNPs with different V% of TEOA. To investigate the fluorescence lifetime of the *N, P*-CNPs(TEOA) charge transfer state with varying concentrations of TEOA (1-5 V%) are excited using a 510 nm laser diode. For 510 nm excitation, the fluorescence time constant of the acquired data is determined using DAS6 decay analysis software integrated with the instrument, which utilizes a fitting Equation 1. Equation-2 is used for fitting the decay traces of 405 nm data¹.

$$I(t) = A + \sum_i B_i \exp\left(\frac{-t}{\tau_i}\right) \quad (1)$$

$$\alpha_i = \frac{B_i}{\sum_{i=1} B_i}$$

and

$$Y(t, \mu, t_p, \sigma) = \sum_{i=1}^n \frac{\alpha_i}{2} e^{\left(\frac{1}{2\tau_1} \left(\frac{\sigma^2}{\tau_i} - 2(t-u) \right) \right)} \left[1 - \operatorname{erf} \left(\frac{\sigma^2 - \tau_i(t-u)}{\sigma \sqrt{2\tau_i}} \right) \right] \quad (2)$$

Where A is the background term, τ_i represents the fluorescence decay, B_i is the pre-exponential value relative to the lifetime component with corresponding amplitudes α_i . The average lifetime (τ_{avg}) is studied with the following equation.

$$\tau_{av} = \frac{\sum_i \alpha_i \tau_i}{\sum_i \alpha_i} \quad (3)$$

To extract the time component from the TA data, kinetic traces were fitted with equation 2 for both pump excitation (400 nm, 530 nm).

Sample	$\lambda_{ex}(\text{nm})$	α_1	τ_1 (ns)	α_2	τ_2 (ns)	τ_{avg} (ns)	χ^2
Pure N, P CNPs	405	0.77	0.44	0.23	4.34	1.32	0.99
N, P-CNPs(TEOA) or 1%V TEOA	405	0.65	0.68	0.35	3.63	1.71	0.99
N, P-CNPs(TEOA) or 1%V TEOA	510	0.64	0.67	0.36	2.16	1.21	0.89

Table S6: Fluorescence lifetime and corresponding amplitudes using 405 and 510 nm diode.

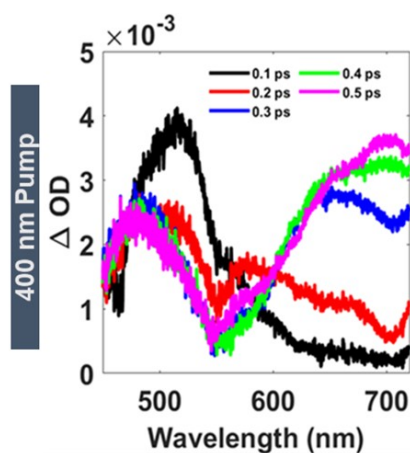


Figure- S20: Spectral traces for *N, P*-CNPs (TEOA) or 1V% TEOA at early time delays.

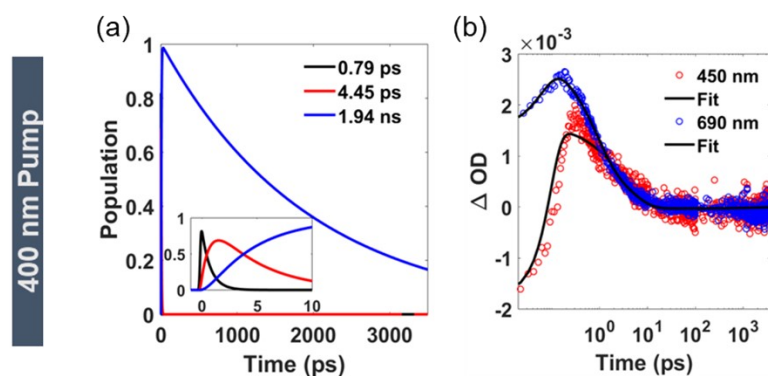


Figure- S21: Femtosecond transient absorption studies of *N, P*-CNPs (TEOA) or 1 V% TEOA, (a) time evolution population and (b) kinetic traces along with fit (in black) to raw data (in scatter) at different select probe wavelengths.

Sample	Signal/Wavelength (nm)	α_1	τ_1 (ps)	α_2	τ_2 (ps)	α_3	τ_3 (ps)	RMS
2V% TEOA (530 nm)	ESA (430)	0.46	0.84	0.26	9.45	0.27	550.0	0.71
	GSB+SE (519)	0.70	1.02	0.25	33.78	0.05	1500.0	0.78
5V% TEOA (530 nm)	ESA (430)	0.50	0.98	0.25	18.26	0.25	609.3	0.95
	GSB+SE (519)	0.51	1.08	0.29	35.41	0.20	1083.0	0.97
2V% TEOA (400 nm)	ESA (460)	0.71	3.50	0.29	58.2	-	-	0.92
	ESA (690)	-0.004	0.94	0.89	2.0	0.10	56.5	0.98
5V% TEOA (400 nm)	ESA (450)	0.72	3.10	0.28	42.9	-	-	0.87

	ESA (690)	-0.56	0.99	0.36	2.1	0.08	37.4	0.98
--	-----------	-------	------	------	-----	------	------	------

Table-S7: TA kinetic fit parameters for varying TEOA content at the different probe wavelengths for 530 and 400 nm excitation.

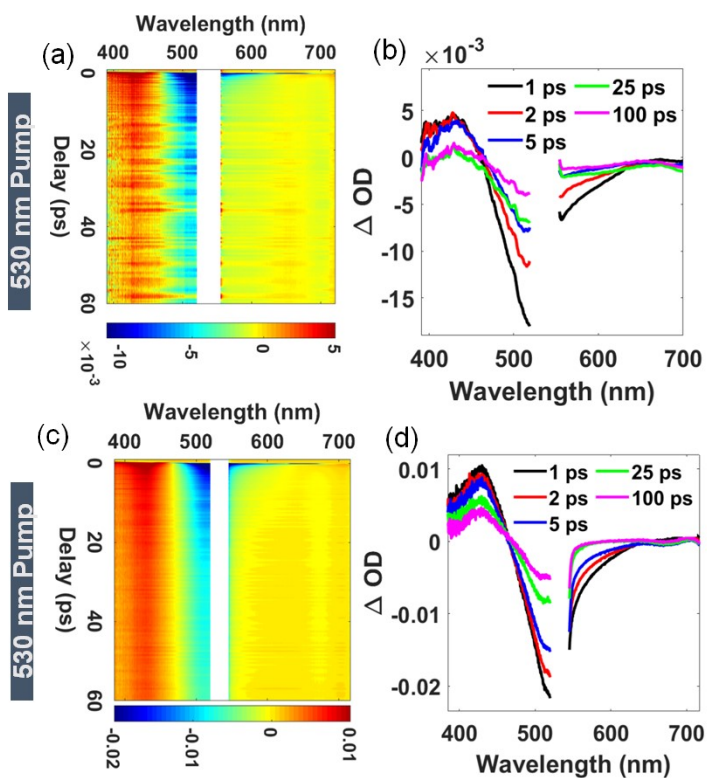


Figure- S22: Femtosecond transient absorption studies of *N, P*-CNPs(TEOA) adduct at higher TEOA conc of 2V% (top row) and 5V% (bottom row) ($\lambda_{pump}=530$ nm): (a, c) transient contour maps, (b, d) spectral traces at the different probe delay.

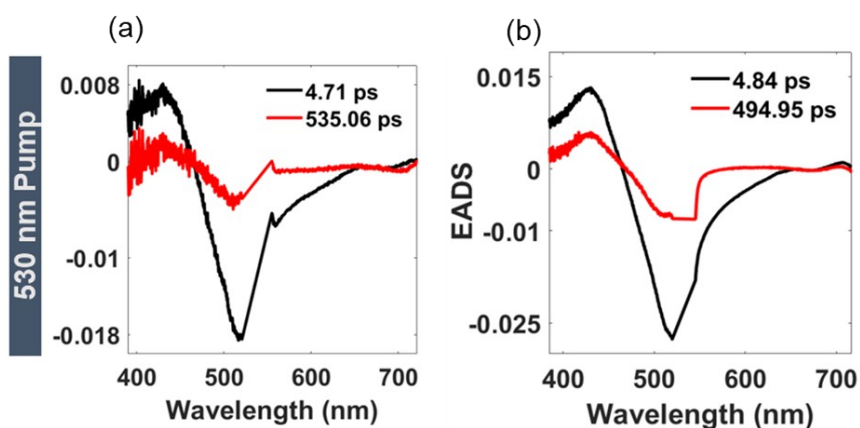


Figure- S23: Femtosecond transient absorption studies of *N, P*-CNPs(TEOA) adduct at higher TEOA conc of 2V% (left column) and 5V% (right column) ($\lambda_{pump}=530$ nm): **(a-b)** evolution-associated decay spectra obtained from global analysis.

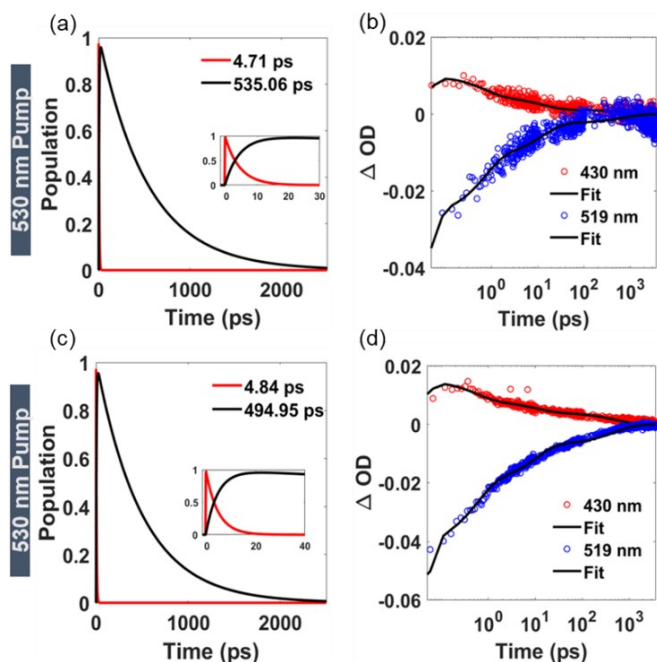


Figure- S24: Femtosecond transient absorption studies of *N, P*-CNPs(TEOA) adduct at higher TEOA conc of 2V% (top row) and 5V% (bottom row) ($\lambda_{pump}=530$ nm): **(a-b)** time evolution population and **(c, d)** kinetic traces along with fit (in black) to raw data (in scatter) at different select probe wavelengths.

Sample	Pump wavelength	τ_1 (ps)	τ_2 (ps)	τ_3 (ps)	RMS
2V% TEOA	400 nm	0.75	4.62	981.6	0.00018
	530 nm	-	4.71	535.06	0.00130
5V% TEOA	400 nm	1.17	7.41	558.4	0.00017
	530 nm	-	4.84	494.95	0.00085

Table- S8: Kinetic fit parameters of fs-TA data obtained from global analysis.

Sample	$\lambda_{\text{ex}}(\text{nm})$	α_1	τ_1 (ns)	α_2	τ_2 (ns)	τ_{avg} (ns)	χ^2
2V% TEOA	405	0.57	0.41	0.43	1.75	0.98	0.99
2V% TEOA	510	0.69	0.51	0.31	1.46	0.80	0.96
5V% TEOA	405	0.66	0.33	0.34	1.57	0.74	0.99
5V% TEOA	510	0.74	0.49	0.26	1.29	0.70	0.87

Table- S9: Fluorescence lifetime and corresponding amplitudes using 405 and 510 nm diode.

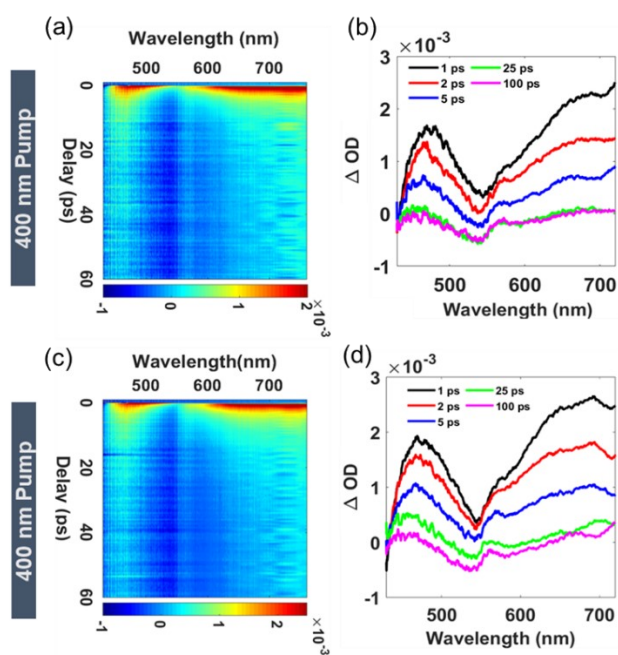


Figure-S25: Femtosecond transient absorption studies of *N, P*-CNPs (TEOA) adduct at higher TEOA concentration of 2V% (top row), 5V% (bottom row) ($\lambda_{pump}=400$ nm): (A, F) transient contour maps, (B, G) spectral traces at the different probe delay.

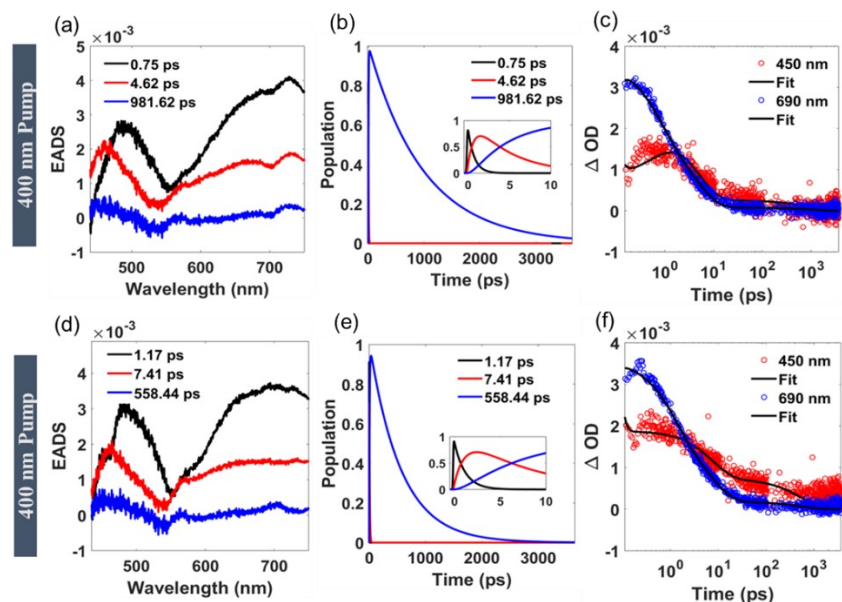


Figure- S26: Femtosecond transient absorption studies of *N, P*-CNPs (TEOA) adduct 2V% (top row), 5V% (bottom row) ($\lambda_{pump}=400$ nm): (a, d) evolution-associated decay spectra obtained from global analysis, (b, e) time evolution population and (c, f) kinetic traces along with fit (in black) to raw data (in scatter) at different select probe wavelengths.

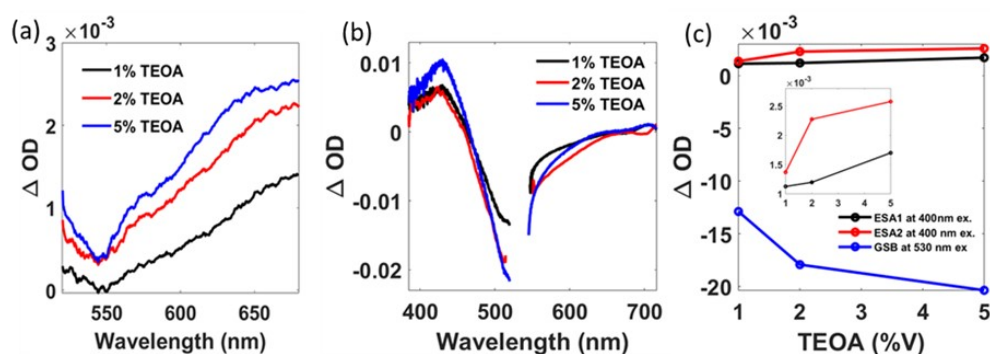


Figure-S27: Spectral traces for *N, P*-CNPs (TEOA) at different concentrations of TEOA at a probe delay of 1 ps corresponding to (a) 400 nm and (b) 530 nm pump excitations, respectively. (c) Variation of maximum intensity of differential absorption with TEOA concentration at ESA1

(460 nm) and ESA2 (690 nm) bands for 400 nm excitation, GSB (519 nm) band for 530 nm excitation.

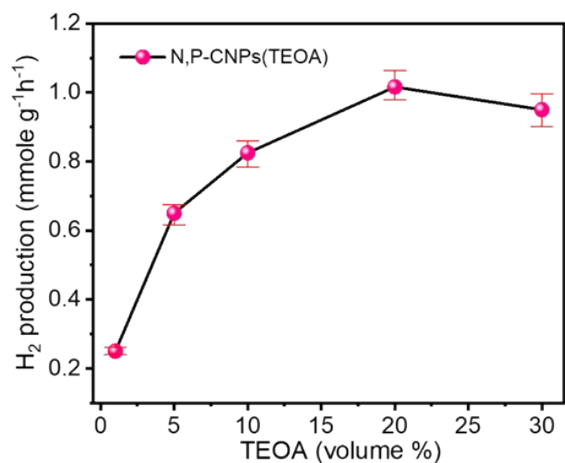


Fig-S28: Photo-catalytic hydrogen generation activities of N, P-CNPs as a function of TEOA concentration (volume %).

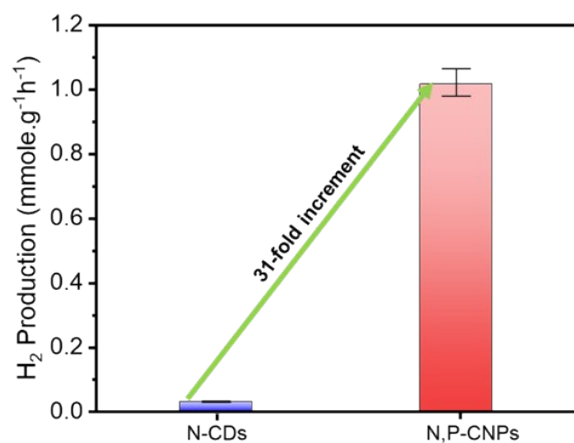


Fig-S29: A comparison of photo-catalytic hydrogen generation activities of N, P-CNPs, and N-CDs at similar TEOA environments.

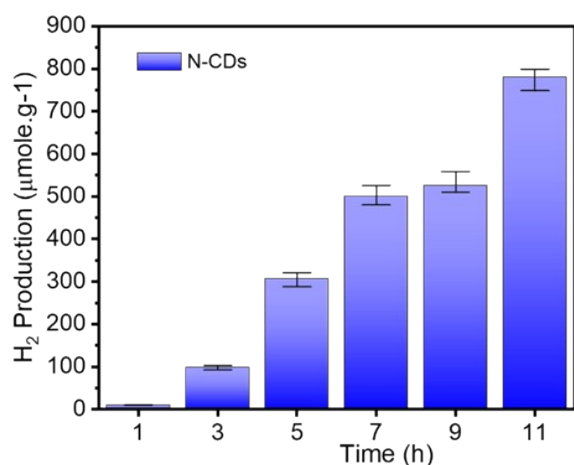


Fig-S30: Time-dependent photo-catalytic hydrogen generation activities of N-CDs.

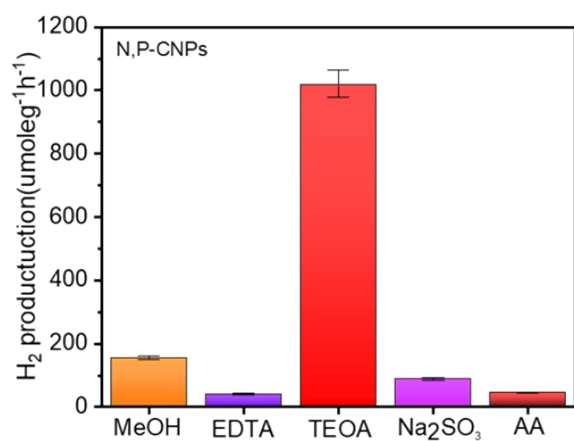


Fig-S31: Solar hydrogen production by N, P-CNPs in the presence of different sacrificial electron donors (SEDs).

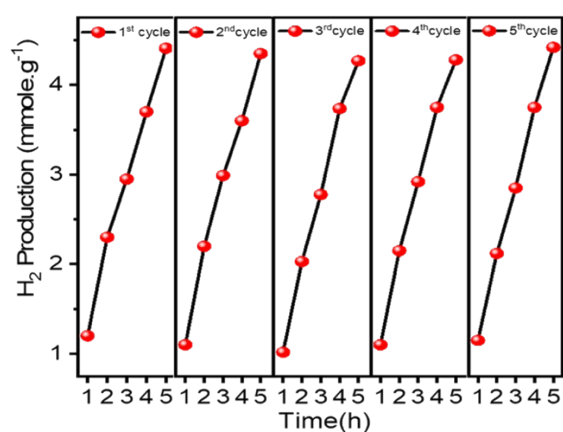


Fig-S32: N, P-CNPs (TEOA) photo-catalyst recycling for solar hydrogen production five times (every five hours).

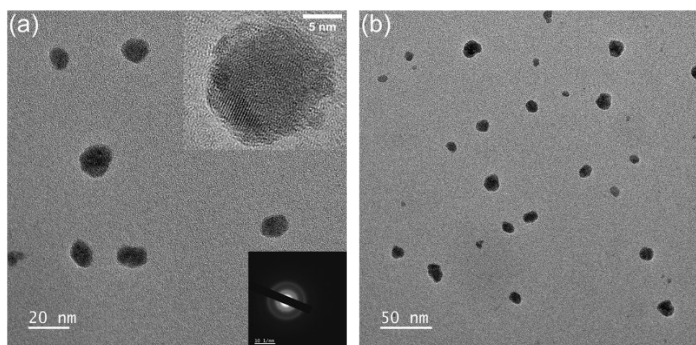


Fig-S33: Structural stability test of *N, P*-CNPs: Post catalytic (10h, without SEDs) morphological analysis using high-resolution (a) and low-resolution (b) TEM study.

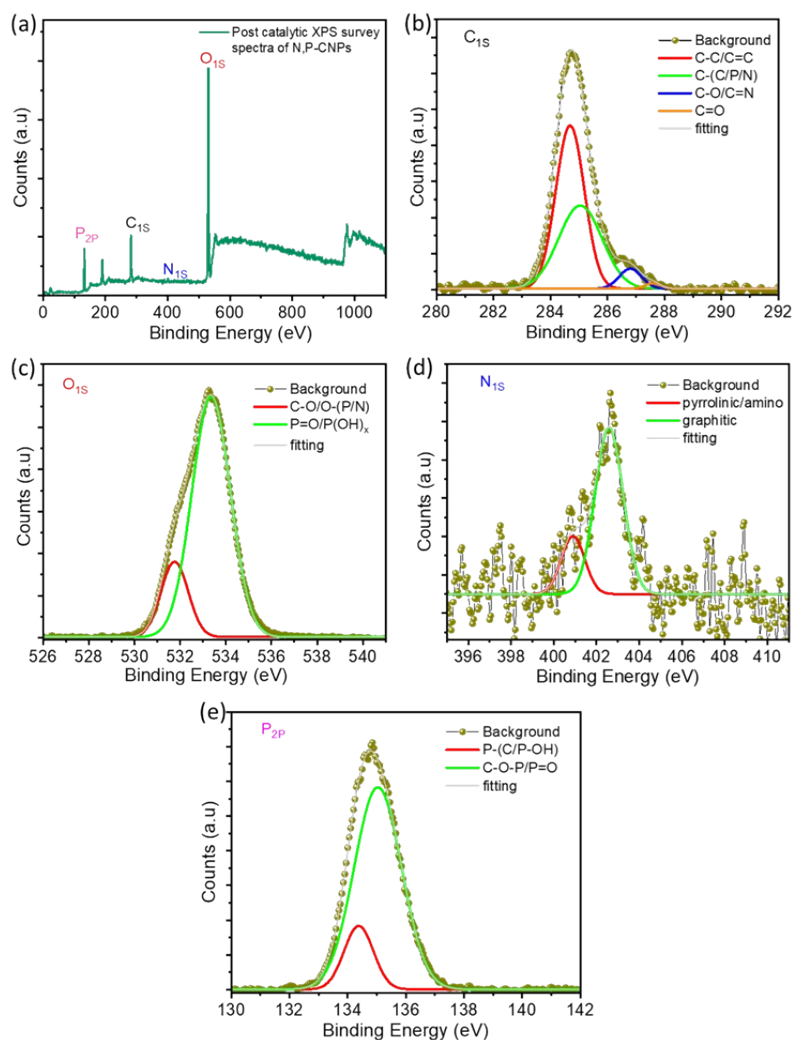
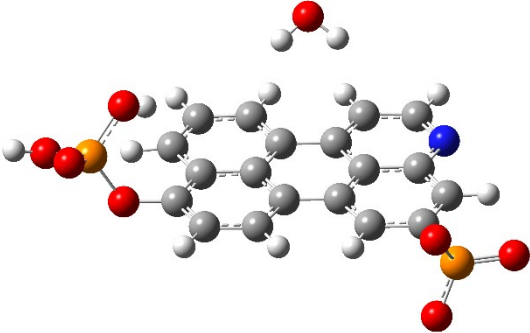
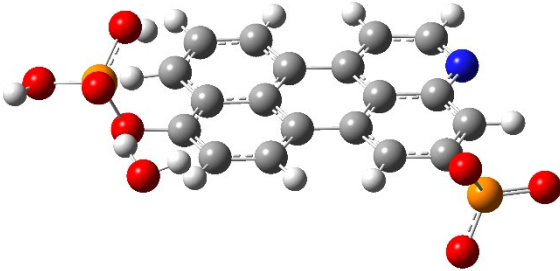
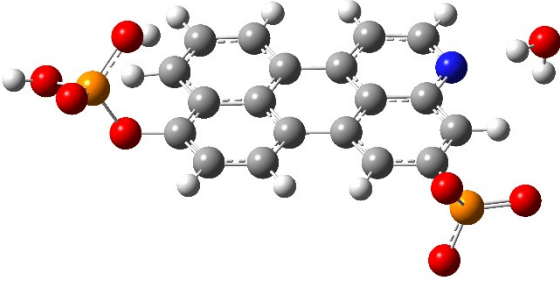


Fig-S34: Structural stability test of *N, P*-CNPs using elemental study (XPS): Post catalytic (10h, without SEDs) XPS survey spectrum (a), High-resolution C_{1s} , High-resolution N_{1s} , High-resolution P_{2p} spectrum, and High-resolution O_{1s} spectrum.

Site	Geometry	ΔG_{ads} (kcal/mol)
site_1		-52.4
site_2		-54.4
site_3		-56.3

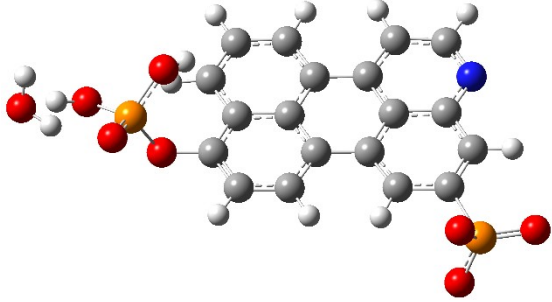
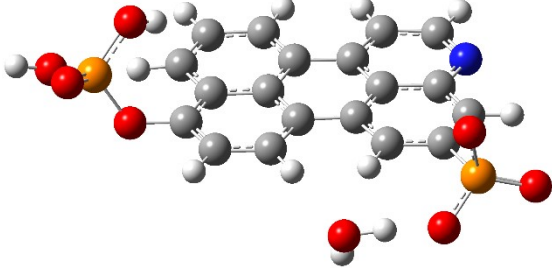
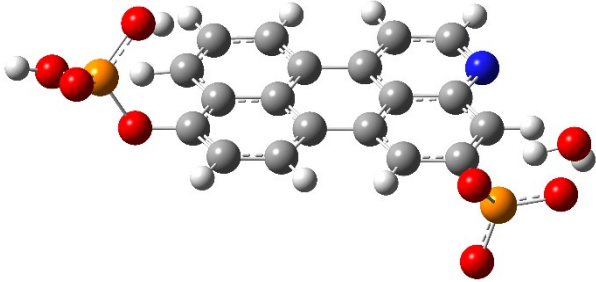
site_4		-60.0
site_5		-67.8
site_6		-68.1

Table-S10: Gibbs free energy (ΔG_{ads}) of adsorbed water on different reactive sites for N, P-CNPs.

SIV. Detailed Characterization

All nanomaterials were morphologically analyzed using a JEOL JEM-F200 TEM instrument with a 200 kV voltage gradient. The TEM images were acquired by dropping significantly diluted samples onto a carbon-coated copper grid with perforations. FTIR (Fourier Transform Infrared Spectroscopy) readings were obtained using the BRUKER TENSOR II. Implementing the Anton Paar & LitesizerTM 500 instrument, the Zeta potentials of the samples were calculated. A smart probe-based Bruker AVANCE NEO Ascend 400 spectrometer is utilized

to obtain ^{31}P -NMR spectra, and the measurements were done at 400MHz. The PHI 5000 Versa Probe-enabled X-ray photoelectron spectrometer (XPS) was utilized to evaluate each sample's surface elemental composition. Raman spectra of the samples were recorded using Renishaw Raman spectrometer equipped with a 785 nm excitation laser source. The UV-visible absorption characteristics of the samples were acquired using a spectrophotometer (Shimadzu, model UV-2550). A Modular Spectrofluorometer, Fluorolog-3 (300 W xenon source), was used to detect the samples' photoluminescence. For the time-resolved photoluminescence decay (TRPL) experiment, an EDINBURGH Life-Spec II model and a 450 nm laser excitation source were used. Besides, the Delatflux TCSPC system from Horiba was employed to examine the details of the N, P-CNPs (TEOA) complex using 405 and 510 nm excitation sources. The excited state dynamics were investigated using Newport's custom-built femtosecond transient absorption spectrometer. All electrochemical studies in this study are carried out using a CHI 760e electrochemical workstation.

References

- (1) Silori, Y.; Chawla, S.; De, A. K, *ChemPhysChem* **2020**, *21* (17), 1908–1917.